Green Chemistry

PAPER

View Article Online
View Journal | View Issue

Cite this: *Green Chem.*, 2024, **26**, 3346

A highly efficient and sustainable catalyst system for terminal epoxy-carboxylic acid ring opening reactions†

Tizian-Frank Ramspoth, *[a] Jitte Flapper,[b] Keimpe J. van den Berg, [b] Ben L. Feringa *[a] and Syuzanna R. Harutyunyan *[a]

Received 6th November 2023,
Accepted 15th January 2024

DOI: 10.1039/d3gc04301k

rsc.li/greenchem

The nucleophilic ring opening of epoxides by carboxylic acids is an indispensable transformation for materials science and coating technologies. Due to this industrial significance, improvements in operational energy consumption and catalyst sustainability are highly desirable for this transformation. Herein, an efficient, environmentally benign and non-toxic halide free cooperative catalyst system based on an iron(III) benzoate complex and guanidinium carbonate is reported. The novel catalyst system shows improved activity over onium halide catalysts under neat conditions and in several solvents, including anisole and ^{n}BuOAc. Detailed mechanistic studies using $FeCl_3$/DMAP as a catalyst revealed the importance of a carboxylate bridged cationic trinuclear μ_3-oxo iron cluster and guanidinium carbonate or DMAP as a carboxylate reservoir due to its superior activity.

Introduction

The formation of β-hydroxyesters derived from the nucleophilic ring opening of epoxides by carboxylic acids is a reaction of high value. Apart from its relevance for accessing drug precursors[1,2] and its occurrence in biologically relevant processes,[3] the transformation is industrially important for the synthesis of monomers for photocurable resins and adhesives[4] as well as for crosslinking reactions.[5,6] Due to this industrial significance for large scale applications, the reaction demands exhaustive optimization towards sustainability. In this regard, research has mainly focussed on replacement of reactants with biofeedstock derived materials.[7–12] However, the design of a broadly applicable and sustainable catalyst system with high activity and compatibility with environmentally benign solvent is necessary to fully exhaust the optimization potential for this invaluable transformation. The origin and environmental fate of the catalyst material from cradle to grave can have a significant impact on a large scale and its activity directly influences the energy consumption of the process.[13,14]

Industrial applications largely employ catalysts such as triethylamine,[15–24] *n*-tetrabutylammoniumbromide[25–34] or triphenylphosphine,[35–44] which can have adverse effects on health,[45–47] aquatic life[46] or tropospheric ozone concentrations[48,49] and often rely on halogenated petrochemical feedstock for their synthesis.[50–53] More benign alternatives such as triethylbenzylammoniumchloride[54–56] are likewise accessed through halogenated precursors[57] and alkali hydroxides,[58,59] alkali carbonates,[60,61] metallic Lewis acids[62,63] or heterogeneous catalysts[64] often have limitations of catalytic activity or chemoselectivity with respect to polyether bond formation.

The need for a sustainable and highly active catalyst system for industrially relevant epoxy-carboxylic acid reactions, which can operate under neat conditions and in environmentally benign solvents, is therefore high.

Cooperative approaches utilizing a Lewis acid (LA) such as $FeCl_3$ or $CrBr_3$ in conjunction with an amine[65] or specifically with pyridine[66] have been reported to achieve enhanced catalytic activity and improved chemoselectivity for this reaction (Scheme 1a and b). The effect is rationalized by simultaneous activation of the epoxide electrophile and carboxylic acid nucleophile through Lewis acidic and basic interactions with the metal salt and the amine, respectively. However, these catalyst systems have not been further explored, as the design of an LA/(L)B cooperative catalyst system is challenging, due to potentially inhibiting interactions between both catalyst components. Furthermore, concerns regarding the environmental fate and the toxicological profile of catalyst components like pyridine[67–69] and triethylamine[48] remain for these systems as well.

[a]*Stratingh Institute for Chemistry, Advanced Research Center Chemical Building Blocks Consortium (ARC CBBC), University of Groningen, Nijenborgh 7, 9747 AG Groningen, The Netherlands. E-mail: s.harutyunyan@rug.nl, b.l.feringa@rug.nl, t.ramspoth@rug.nl*

[b]*Department Resin Technology, AkzoNobel Car Refinishes BV, 2171 AJ Sassenheim, The Netherlands*

† Electronic supplementary information (ESI) available. See DOI: https://doi.org/10.1039/d3gc04301k

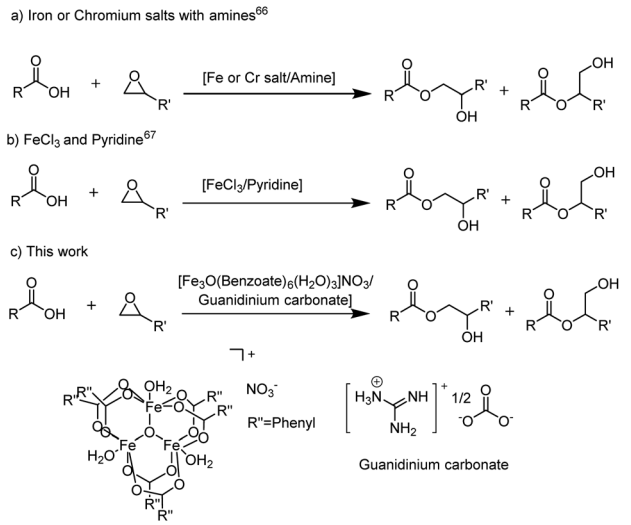

Scheme 1 Reported LA/LB cooperative catalyst systems for the nucleophilic ring opening of epoxides by carboxylic acids; (a) iron or chromium salts in conjunction with amines,[65] (b) $FeCl_3$/pyridine[66] and (c) this work: the ($[Fe_3O(benzoate)_6(H_2O)_3]NO_3$)/guanidinium carbonate catalyst system.

In this work, we have developed an effective, sustainable and easily accessible cooperative catalyst system, composed of $[Fe_3O(Benzoate)_6(H_2O)_3]NO_3$ and guanidinium carbonate (Scheme 1c). Its constituents are naturally abundant, considered environmentally friendly and are already accessible *via* industrially established routes without the involvement of halogenated compounds. Additionally, this catalyst system outcompetes state-of-the-art catalysts in industrially common solvents, in green solvent alternatives and under neat conditions, which further contributes to a more sustainable reaction profile through reduction of the reaction time and temperature.

Results and discussion

In our quest to find a sustainable catalyst system for epoxy-carboxylic acid ring opening reactions we decided to focus on LA/LB cooperative systems as the most promising candidates to catalyse the target transformation. We started by screening metal-based Lewis acids in a model reaction of benzoic acid (**1a**) with 1,2-epoxyhexane (**2**) in toluene at reflux (Table 1). Under these conditions, $Zr(acac)_4$ (Table 1, entry 2) and $FeCl_3$ (Table 1, entry 3) showed the highest catalytic activity. The performance of iron(III) acetylacetonate and iron(III) nitrate salts was inferior compared to that of the chloride salt (Table 1, entries 4 and 5). Other metal salts, such as $AlCl_3$, also showed lower catalytic activity and were limited by solubility (Table 1, entry 7 and ESI 3†), while triflate salts promoted epoxide homopolymerization instead (Table 1, entries 8 and 9).

Following LA catalyst experiments, the screening of nitrogen-based Lewis bases was performed as well under the same reaction conditions (Table 1, entries 10–13). This led to the identification of 4-dimethylaminopyridine (DMAP) as the most potent structure (Table 1, entry 10).

Table 1 Optimisation results for the model reaction of **1a** and **2**

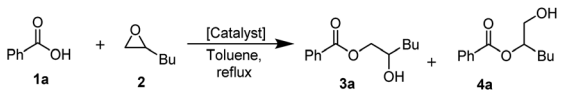

Entry	Catalyst [2 mol%]	Conv., **3a** + **4a**[a] [%]
1	None	3
2	$Zr(acac)_4$	66
3	$FeCl_3$	64
4	$FeCl_3$ (1 mol%)	32
5	$Fe(NO_3)_3 \cdot 9\ H_2O$	52
6	$Fe(acac)_3$	37
7	$AlCl_3$	7
8	$Fe(OTf)_3$	n.d.
9	$Sc(OTf)_3$	n.d.
10	DMAP	63
11	DMAN[b]	13
12	Pyridine	42
13	2,6-Lutidine	11
14	$FeCl_3$/DMAP [1/1]	82
15	$FeCl_3$/pyridine [1/1]	78
16	$FeCl_3$/2-picolinic acid [1/1]	40
17	$FeCl_3$ + L-proline [1/1]	22
18	$FeCl_3$/2,2′-bipyridyne [1/1]	42
19	$FeCl_3$/4,4′-bipyridyne [1/1]	58
20	$FeCl_3$/DIPEA [1/1]	71
21	$FeCl_3$/DMAN [1/1]	70
22	$FeCl_3$/Barton's base [1/1]	83

Reaction conditions: **1a** (1.5 mmol), **2** (1.5 mmol), reflux, 3 h. [a] Determined by ^{1}H-NMR spectroscopy of **1a** and **3a** + **4a**, regioisomer ratios (**3a**/**4a**) range from 66 : 33 to 74 : 26. [b] DMAN = 1,8-bis(dimethylamino)naphthalene.

We combined equal amounts of the best performing stand-alone LA and LB catalysts ($FeCl_3$ and DMAP) and confirmed that the duo catalytic system surpasses the catalytic activity of the 2-fold amount of either of its components as stand-alone catalysts (Table 1, entry 14). Toluene was identified as the most optimal solvent for this transformation. Running the reaction in more polar solvents resulted in either lower catalytic activity or decreased chemoselectivity (ESI, 4†). The effect of the LA/LB ratio on the catalytic performance of the DMAP/$FeCl_3$ combination was studied and it was found that there is a marginal increase in conversion for higher LA/LB ratios (ESI, 5†).

Next, we decided to re-evaluate the nature of the LB combined with $FeCl_3$ (Table 1, entries 15–22). The results revealed that the DMAP/$FeCl_3$ catalyst system performs slightly better than the previously reported pyridine/$FeCl_3$ catalyst, while bidentate ligands such as picolinic acid, L-proline and 2,2′-bipyridine performed worse than 4,4′-bipyridine, and sterically hindered bases such as *N*,*N*-diisopropylethylamine (DIPEA), DMAN, and Barton's base performed well in conjunction with $FeCl_3$ (for the full set of screening data, see ESI 3†).

To understand the precise role of DMAP, we performed the reaction using higher loadings of it as a standalone catalyst (Table 2). For 25% and 50 mol% of DMAP loading (Table 2, entries 1 and 2), the conversion towards the *β*-hydroxyester pro-

Table 2 Reaction of (**2**) and DMAP in the presence of **1a**

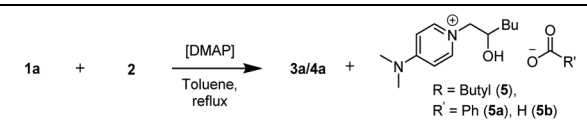

Entry	**DMAP** [mol%]	(**3a** + **4a**)[a] [%]	Yield, **5b** [b] [%]
1	[25]	74	n.d.
2	[50]	51 (53)	52
3	[75]	49	n.d.

Reaction conditions: **1a** (1.5 mmol), **2** (1.5 mmol), reflux, 20 h. [a] Determined by GC-FID; the value in parentheses corresponds to the isolated yield. [b] Isolated yield based on DMAP. Product **5** was also observed in entries 1 and 3 but the yield was not determined.

ducts (**3a** + **4a**) reached 74% and 51% respectively. With 50 mol% of DMAP, 53% of β-hydroxyester products (**3a** + **4a**) were isolated. Additionally, an ionic ring opening product (ROP), which formed *via* the reaction of DMAP with 1,2-epoxyhexane (**2**), was isolated as a formate salt (ROP-FA, **5b**) after reverse phase column chromatography. Employing 75% of DMAP led to a conversion of 49% of (**3a** + **4a**) (Table 2, entry 3).

No formation of ROP (**5**) was observed in the absence of benzoic acid. Next, we screened ROP-FA (**5b**) as a stand-alone catalyst in combination with $FeCl_3$ and achieved comparable catalytic activity to DMAP (ESI, 8†). Similar structures, resulting from the nucleophilic addition of an amine to an epoxide, have been previously proposed to be mechanistically relevant for the amine catalysed epoxide ring opening with carboxylic acids.[7] Employing ROP-FA (**5b**) as a substrate with benzoic acid (**1a**) did not lead to product formation in the presence of DMAP, DMAP/$FeCl_3$ or sodium benzoate (ESI, 8†).

Upon leaving a reaction mixture containing $FeCl_3$/DMAP at room temperature, dark red, rod-shaped crystals were formed. We were unable to obtain a high-resolution structure by X-ray crystallography, but core structural features (ESI, 14†) have been identified by NMR-spectroscopy and HRMS. The obtained material consists of a cationic μ_3-oxo trinuclear iron cluster, bridged by six benzoates, similar to the structures reported in the literature.[70–72] ^{1}H- and ^{13}C-NMR spectroscopy and HRMS confirmed the presence of ROP species in the crystal structure. The crystals exhibited catalytic activity similar to the $FeCl_3$/DMAP system (Table 3, entry 1). To understand the role of the cationic μ_3-oxo trinuclear benzoate type cluster, we independently prepared clusters **7**[71] and **8** and tested them in our reaction. Cluster **7** showed almost identical catalytic activity to $FeCl_3$ (Table 3, entry 2 *versus* Table 1 entry 4). Combination of **7** with DMAP and cluster **8** alone exhibited comparable catalytic performance to the $FeCl_3$/DMAP system (Table 3, entries 2–4).

Next, we confirmed the presence of an equilibrium between the benzoate ligands coordinated to the cluster and free benzoic acid in solution, by observing a scrambled β-hydroxyester product when using 2,3,4,5,6-deuterobenzoic acid as a substrate in the presence of the $[Fe_3O(Benzoate)_6(H_2O)_3]NO_3$

Table 3 Synthesis of iron(III) cluster complexes and evaluation of their catalytic activity

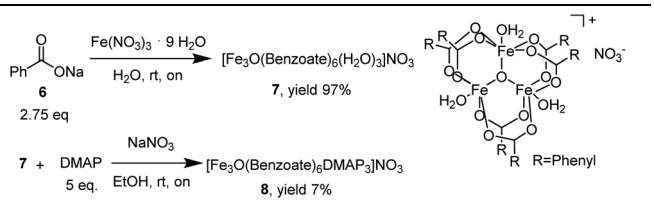

Entry	Catalyst [0.33 mol%]	Conv., **2**[a] [%]	**3a**/**4a**[b]
1	$Fe_3O(benzoate)_6(ROP)_3Cl$[c]	73	2.7
2	**7**	33	2.4
3	**7**/DMAP[d]	87	2.6
4	**8**	83	2.6

Reaction conditions: **1a** (1.5 mmol), **2** (1.5 mmol), reflux, 3 h. [a] Determined by GC-FID, with mesitylene as the external standard. [b] Determined by ^{1}H-NMR signals of both regioisomers of the product. [c] Assumed structure. [d] The ratio 7/DMAP = 0.33 mol%/1 mol%.

(**7**)/DMAP catalyst system (ESI, 13†). Following this, the electronic and steric effects of the benzoic acid substrate have been investigated (Scheme 2).

The products derived from *p*-CN (**3d**/**4d**; 69 : 31) as well as *p*-methoxy (**3e**/**4e**; 70 : 30) substituted benzoic acids were isolated in comparable yields to **3a**/**4a** (70 : 30), indicating that the electronic properties of the carboxylic acid have a minor effect on the reaction outcome. However, significantly lower yields were obtained for the products with bulkier aromatic substituents, such as *p*-^{t}butyl (**3g**/**4g**; 72 : 28) or *p*-phenyl (**3h**/**4h**; 63 : 37) (Scheme 2). Furthermore, comparable yields and regioisomer ratios have been obtained for an extended substrate

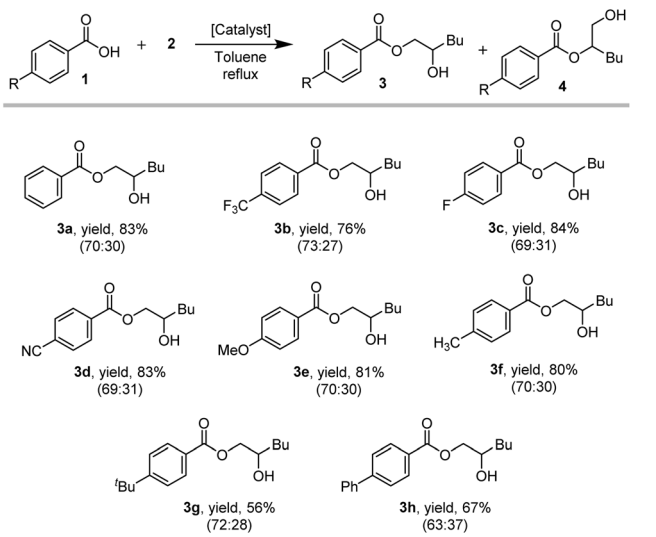

Scheme 2 Substrate scope of *para*-substituted benzoic acids with 1,2-epoxyhexane. Reaction conditions: **1** (1.5 mmol), **2** (1.5 mmol), reflux, overnight; 1 mol% $FeCl_3$ + 1 mol% DMAP. Combined isolated yields of both regioisomers (**3** + **4**) is given; only the major isomer is depicted for clarity, ratio of **3** : **4** depicted in parentheses.

scope including aliphatic carboxylic acids and an aromatic epoxide for $FeCl_3$/DMAP and TBAB as catalysts (ESI, 14†).

Next, we compared the conversions of different *para*-substituted benzoic acids (*p*-H, *p*-CF_3, *p*-CH_3) after 3 h of reaction time. From the assessed benzoic acids, the most nucleophilic *p*-toluic acid (**1f**) reacted fastest, followed by benzoic acid (**1a**) and *p*-CF_3 benzoic acid (**1b**). Although the trend is marginal, it suggests an equal or slightly higher reactivity for more nucleophilic carboxylic acids (ESI, 9†).

However, in a direct competition experiment, employing *p*-CF_3, *p*-CH_3 and *p*-H benzoic acid in equal amounts as substrates (totalling one equivalent of acid substrate w.r.t. **2**), a different result was observed (Table 4). The *p*-CF_3 benzoic acid (**1b**) reacted preferably in this scenario: after 20 minutes, 39% of **1b** was consumed, while more than 90% of benzoic-(**1a**) and *p*-toluic acid (**1f**) were still present in the reaction medium (Table 4, entry 1). After 3 h, **1b** was completely consumed, while 27% and 42% of **1a** and **1f** were still present, respectively (Table 4, entry 2). After 21 h, all three carboxylic acid substrates were completely consumed (Table 4, entry 3), although a decrease in ^{1}H-NMR yield was observed, likely due to transesterification or other side processes.

In order to gain a conclusive mechanistic insight, we studied the reaction kinetics. We determined the reaction orders in catalysts and substrates for the $FeCl_3$/DMAP system and DMAP as a standalone catalyst (for the results with $FeCl_3$ as a standalone catalyst see ESI 18–21†) using the visual kinetics analysis method described by Burés *et al.*[73] Catalyst degradation and product inhibition effects were ruled out by performing "same excess" experiments at two different starting concentrations for each of the catalyst systems (ESI, 18†). For the $FeCl_3$/DMAP system, the reaction is zero order in benzoic acid (Table 5), while for the DMAP catalysed reaction, a half order in benzoic acid (**1a**) was found. For both the DMAP catalysed reaction and the cooperative $FeCl_3$/DMAP system, a first order in epoxide and the catalyst was determined.

The results indicate a correlation between the reactivity and acidity of the nucleophiles. In a direct competition experiment, the observed selectivity across the three acids is contrary to the observed conversion tendencies of the *p*-substituted acids as standalone substrates (ESI, 9†). The slower reacting *p*-CF_3 benzoic acid (**1b**) appears to be consumed faster than its more electron rich analogues (**1a**, **1f**), which suggests that the ionic ROP and potentially unreacted DMAP are acting predominantly as a base. In alignment with the change in the order of the acid from 0.5 in the DMAP catalysed reaction to 0 when using the $FeCl_3$/DMAP catalyst system, we propose that the main purpose of the Lewis basic species is to create a reservoir of carboxylates *via* deprotonation of the carboxylic acid.

The carboxylate nucleophile is consumed from within this reservoir, whereas the selectivity in a direct competition experiment between different carboxylic acid substrates is determined by the relative concentrations of the respective carboxylates present in the reaction medium. As the amount of base is limited, the acid with the highest pK_a is the dominant carboxylate in the reservoir, leading to the observed preference in acid consumption during the ring opening of **2**.

Based on the acquired data, a mechanistic proposal for this cooperative catalytic transformation is presented in Scheme 3.

Formation of **I** can proceed *via* coordination of carboxylic acid in the presence of ROP/DMAP as a suitable ligand to occupy the remaining coordination vacancies. Ligand exchange in favour of the epoxide gives rise to species **II**, where both substrates coordinate to the catalyst. The released ROP/DMAP deprotonates a carboxylic acid molecule outside of the coordination sphere of the catalyst, followed by exchange of the counter ion, leading to species **III**. In the following step, either an intramolecular nucleophilic attack of a carboxylate ligand on the coordinated epoxide, accompanied by a concerted regeneration of the catalytically active cluster structure from the carboxylate which is present as a counter ion (Scheme 3, a) or a direct outer sphere type attack of the carboxylate counterion (Scheme 3, b) occurs. This leads to the formation of neutral species **IV**, with the product coordinated to the cluster *via* its generated alcoholate moiety. Upon protonation, the *β*-hydroxyester product is released and species **I** is regenerated.

Steps III and IV are expected to be rate determining, as no product inhibition is observed and the previous steps are characterized by zero order behaviour of the carboxylic acid and its acidity dependent selectivity.

Considering drawbacks of the $FeCl_3$/DMAP catalyst system, such as the corrosiveness of the iron source and the toxicity, the detrimental biodegradability and the negative impact of DMAP on aquatic life,[74] we decided to explore sustainable alternatives based on the above mechanistic proposal. Based

Table 4 *In situ* competitive experiment with *para*-substituted benzoic acids

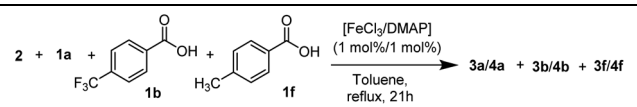

Time	**1a** [a]	(**3a** + **4a**)[b]	**1b**[a]	(**3b** + **4b**)[b]	**1g**[a]	(**3g** + **4g**)[b]
0.33 h	7	7	39	30	5	6
3 h	73	75	100	100	58	59
21 h	100	99	100	93	100	92

[a] Conversions and formation of **1** in [%] determined by ^{1}H-NMR of the crude. [b] Conversions and formation of (**3** + **4**) in [%] determined by ^{1}H-NMR of the crude. **2**/**1a**/**1b**/**1f** = 1/0.33/0.33/0.33 eq. in toluene, reflux.

Table 5 Reaction orders in components by visual time normalization analysis.[18]

		Reaction order in		
Entry	Catalyst	**1a**	**2a**	Catalyst
1	$FeCl_3$/DMAP (1 : 1)	0	1	1
2	DMAP	0.5	1	1

Reaction conditions: toluene, reflux, oN.

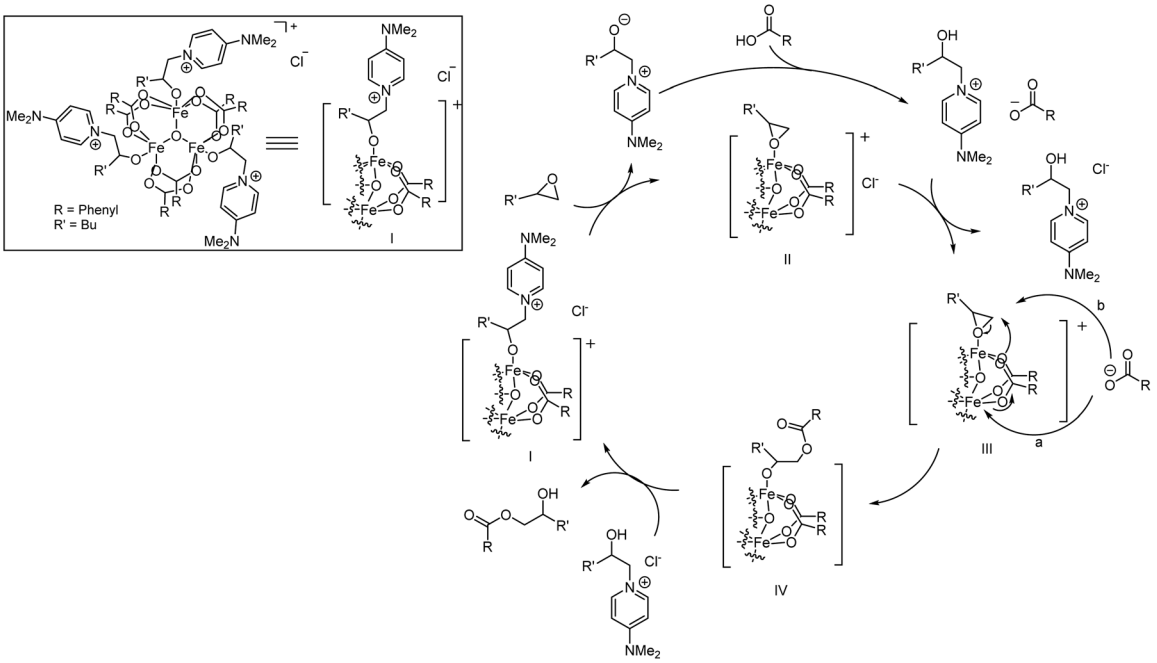

Scheme 3 Proposed catalytic cycle for the $FeCl_3$/DMAP catalyzed nucleophilic ring opening reaction of epoxides with carboxylic acids.

on our results, $FeCl_3$ can be readily replaced by the $[Fe_3O(Benzoate)_6(H_2O)_3]NO_3$ cluster (**7**), which avoids potential HCl formation. As DMAP is proposed to increase the reactivity of the nucleophile *via* formation of a carboxylate based ionic species, a suitable surrogate would have to combine the ability to irreversibly deprotonate the carboxylic acid with high stability of the formed cation, in order to promote the reaction of the carboxylate. We hypothesised that the naturally ubiquitous guanidine[75] would be a proficient substitute to achieve high catalytic activity in conjunction with the iron(III) benzoate cluster (**7**), due to its high basicity and the stability of the corresponding cation.[76] As guanidine reacts with atmospheric water and CO_2,[77,78] guanidinium carbonate (GC) was used. We were delighted to see that GC exhibited equally high activity in conjunction with $[Fe_3O(Benzoate)_6(H_2O)_3]NO_3$ (**7**) as the initial $FeCl_3$/DMAP system under model conditions (Table 6, entries 1 and 2). Interestingly, unlike DMAP, GC has no significant effect on the reaction progress when employed as a standalone catalyst (Table 6, entry 3). The regioisomeric ratios observed for both cooperative catalyst systems are in alignment with the findings reported for the $FeCl_3$/DMAP system (Scheme 2).

To render the system more environmentally friendly, we explored anisole and *n*-butylacetate (^{n}BuOAc)[79] as alternative solvents (Table 7). The catalytic activity of our **7**/GC catalyst system in anisole at 115 °C was comparable to that of its performance in toluene at reflux and it slightly improved in ^{n}BuOAc (Table 7, entry 1). In contrast, the activity of the $FeCl_3$/DMAP system, other common ammonium salts and PPh_3 was worse in both solvents (Table 7, entries 2–5). Tetraphenylphosphoniumbromide (PPh_4Br), on the other hand, showed similar activity to **7**/**GC**, both in anisole and

Table 6 Catalytic performance of guanidinium carbonate (GC) as a substitute for DMAP in the model reaction of **1a** and **2**

			Conv. [%], 1 h		Conv. [%], 3h	
Entry	Catalyst	[mol%]	**1a**[a]	**2**[b]	**1a**[a]	**2**[b]
1	**7**/GC[c]	[0.33/1]	57 (69 : 31)	53	86	84
2	$FeCl_3$/GC	[1/1]	57 (69 : 31)	58	83	82
3	GC[c]	[2]	n.d.	n.d	9	9

Reaction conditions: **1a** (1.5 mmol), **2** (1.5 mmol), reflux in toluene. [a] Determined by ^{1}H-NMR spectroscopy. [b] Determined by GC-FID. [c] GC = guanidinium carbonate. Regioisomeric ratios for entries 1 and 2 are 69 : 31 after 20 h.

Table 7 Performance of relevant catalyst systems in the model reaction of **1a** and **2** using anisole and butyl acetate as solvents

			Conv. [%], 1 h in Anisole		Conv. [%], 1 h, in ^{n}BuOAc	
Entry	Catalyst	[mol%]	**1a** [a]	**2** [b]	**1a** [a]	**2** [b]
1	**7**/GC[c]	0.33/1	51	52	66	63
2	$FeCl_3$/DMAP	1/1	30	30	41	43
3	TBAB	2	19	17	26	27
4	Et_3NBn	2	19	20	24	27
5	PPh_3	2	20	19	16	11
6	PPh_4Br	2	47	52	55	53

Reaction conditions: **1a** (1.5 mmol), **2** (1.5 mmol), 115 °C in anisole or ^{n}BuOAc, [a], [b], and [c] are the same as in Table 6; regioisomeric ratios after 20 h are within the range of 68–32 to 73–27 (for details see the ESI†).

^{n}BuOAc (Table 7, entry 6); however, it shares sustainability disadvantages with the other onium salts, due to its synthesis pathway.[80] The regioisomeric ratios observed after reaction completion were comparable across all tested catalyst systems. In addition, the activity results obtained in (1-methoxy-2-propyl) acetate as a solvent were comparable to the catalyst performances observed in anisole (ESI, 23†).

Next, we looked into the recyclability of the 7/GC catalyst system (Fig. 1). Re-addition of substrates **1a** and **2** to a reaction performed in anisole in the presence of the 7/GC catalyst system after 16 h showed catalytic activity similar to a standard run (79% *vs.* 82% conversion of **2**, 3 h). The recycled catalyst material was isolated in 72% yield through precipitation (assuming guanidinium benzoate formed) from reaction mixtures after 16 h. The recycled material showed a slight drop in the activity (74% *vs.* 82% conversion of **2**, 3 h). In terms of recyclability, 7/GC is advantageous over the $FeCl_3$/DMAP and $FeCl_3$/pyridine system, both of which contain a liquid catalytic component (DMAP forms the liquid ionic species **5** under reaction conditions). This non-volatile character has also operational benefits for large scale industrial applications.

To demonstrate the industrial applicability further, the catalyst system was tested in the synthesis of 2-hydroxy-3-phenoxypropyl methacrylate (**11**), a common structural motif in dental composites[81] and photosensitive resins.[82] When the reaction was performed neat at 65 °C, the $[Fe_3O(Benzoate)_6(H_2O)_3]NO_3$(7)/GC system was superior to currently employed catalysts such as TBAB[83] or triethylamine (Et_3N).[81] Importantly, it performed significantly better than the other common alternative onium halide catalysts tested, including PPh_4Br (Table 8, entries 1–6). After 3 hours, the acid was almost completely consumed by the 7/GC catalyst, whereas TBAB led to 47% of product formation and PPh_4Br reached 60% conversion to the product in the same time period.

For all tested catalysts, the depicted isomer is the major product and only traces of side product formation have been observed.

We opted to conclude this study with an estimation of the sustainability benefit of the $[Fe_3O(Benzoate)_6(H_2O)_3]NO_3$/guanidinium carbonate system. The main advantage of the introduced catalyst system comes from its higher activity under neat conditions and in green solvent alternatives, compared to the largely utilized onium halide and amine catalysts. Additionally, current information suggests that 7/GC is more environmentally benign than other common catalysts, including DMAP and pyridine, considering the toxicological profiles, synthesis pathways and environmental fates. The iron catalyst component is readily synthesized by ligation of $Fe(NO_3)_3{\cdot}9H_2O$ as a halogen free iron precursor, with sodium benzoate in water. The synthesis was successfully conducted on a gram scale. Benzoic acid, industrially produced *via* oxidation of toluene,[84,85] which has in itself still limited accessibility through renewable resources,[86–88] is abundantly present in biomass (*e.g.* plants, fruits, styrax tree).[89] It is, like sodium benzoate, used as a food additive.[90] The iron complex can be isolated almost quantitatively *via* precipitation and washing with water. The expected side products are sodium nitrate, used as a fertilizer,[91] and nitric acid, a reactant for the synthesis of the iron precursor.[92] The carbonate salt of guanidine, an abundant motif in nature[93,94] that can be accessed photosynthetically,[95] is generated as a side product in the pyrolysis of the metabolic waste product urea in the presence of water and CO_2 in the synthesis of melamine.[96–98] It is already used as an ingredient in hair relaxer formulations.[99] Based on the current assessment of regulatory needs conducted by the European Chemicals Agency (ECHA), guanidine carbonate is unlikely to pose risks of toxicity or bioaccumulation and does not require further regulatory risk management[100] in contrast to various issues associated with the use of TBAB[46,49,50] and other common catalysts (see ESI 27†).

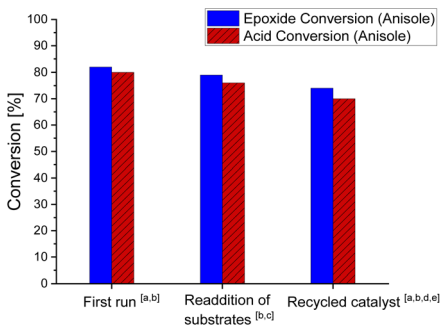

Fig. 1 Reaction conditions: **1a** (4.5 mmol), **2** (4.5 mmol), 0.33/1 mol% **7**/GC, reflux in toluene, and v = 9 mL, [a]determined by ^{1}H-NMR spectroscopy, [b]determined by GC-FID, [c]re-addition to reaction after 16 h [d]equal isolated mol ratio (0.33/1) of $[Fe_3O(Benzoate)_6(H_2O)_3]NO_3$ and guanidinium benzoate assumed, and [e] **1a** (1.5 mmol), **2** (1.5 mmol), and v = 3 mL.

Table 8 Performance of different catalysts in the synthesis of 2-hydroxy-3-phenoxypropyl methacrylate (**11**)

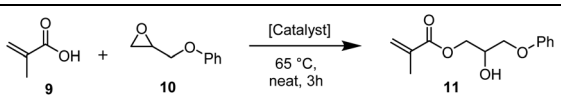

9 10 11

			11[a] [%]	
Entry	Catalyst	Amount [mol%]	1 h	3 h
1	7/GC[b]	[0.33/1]	59	88
2	TBAB	[2]	24	47
3	Et_3N	[2]	3	8
4	Et_3NBn	[2]	22	48
5	PPh_3	[2]	26	51
6	PPh_4Br	[2]	36	60

Reaction conditions: **9** (1.5 mmol), **10** (1.5 mmol), 65 °C. [a] Determined by ^{1}H-NMR spectroscopy. [b] GC = guanidinium carbonate. For all tested catalysts, only traces of side products have been observed.

Conclusions

In this work, we have identified $[Fe_3O(Benzoate)_6(H_2O)_3]NO_3$(7)/guanidinium carbonate as a highly active, non-volatile,

sustainable and non-toxic, halide free cooperative catalyst system for the ring opening reaction of terminal epoxides with carboxylic acids. This system has been demonstrated to be superior to currently employed catalysts in the synthesis of 2-hydroxy-3-phenoxypropyl methacrylate at 65 °C under solvent free conditions. In addition, $[Fe_3O(benzoate)_6(H_2O)_3]NO_3$/guanidinium carbonate proved to be highly active in toluene and 1-methoxy-2-propylacetate and no significant loss of activity was observed when switched to anisole or nBuOAc as a greener solvent alternative. Furthermore, its recyclability has been demonstrated in anisole. The development resulted from detailed mechanistic studies of the $FeCl_3$/DMAP catalyst system, which led to identification of a cationic carboxylate bridged μ_3-oxo trinuclear iron cluster and a basic ionic species formed *via* nucleophilic ring opening of the epoxide by DMAP as catalytically active structures. The presented data support a mechanistic pathway operating *via* a cooperative interaction of the DMAP/ionic species and the iron(III) benzoate cluster, allowing the substitution of $FeCl_3$ with $[Fe_3O(Benzoate)_6(H_2O)_3]NO_3$ and replacement of DMAP by guanidinium carbonate.

Author contributions

T.-F. R. designed the project, carried out the research, visualised and analysed the data and prepared the original manuscript draft. S. R. H. conceptualized and supervised the research project with contributions from B. L. F, K. v. d. Berg. and J. F. All authors commented on the final manuscript.

Conflicts of interest

There are no conflicts to declare.

Acknowledgements

This work is part of the Advanced Research Center for Chemical Building Blocks Consortium,ARC CBBC, which is co-founded and co-financed by the Dutch Research Council (NWO) and the Netherlands Ministry of Economic Affairs and Climate Policy. The authors thank Renze Sneep for high resolution mass spectrometry measurements.

References

1 Y. Luo, Y. Zhang, P. Zhou, Y. He, H. Zhu, X. Li, X. Wu and H. Liu, Preparation method for 3-chloro-2-hydroxy propyl aromatic acid ester, CN108623461A, 2018, A China National Intellectual Property Administration.
2 M. R. Monaco, S. Prévost and B. List, *Angew. Chem., Int. Ed.*, 2014, **53**, 8142–8135.
3 M. Arand, H. Wagner and F. Oesch, *J. Biol. Chem.*, 1996, **8**, 4223–4229.
4 L. Zhou, Y. Song, P. Wang and H. Chen, Efficient synthesis method of hydroxypropyl methacrylate, CN114634414A, 2022, A China National Intellectual Property Administration.
5 S. Thomas, C. Sinturel and R. Thomas, *Micro and Nanostructured Epoxy/Rubber Blends*, *Wiley-VCH*, 2014.
6 M. J. Gadman, J. J. Florio and M. C. Salvi, *CoatingsTech*, 2023, 18–31.
7 S. P. Amaud, N. M. Malitowski, K. M. Casamayor and T. Robert, *ACS Sustainable Chem. Eng.*, 2021, **9**, 17142–17151.
8 S. Wang, J. Dai, N. Teng, J. Hu, W. Zhao and X. Liu, *ACS Sustainable Chem. Eng.*, 2020, **8**, 16842–16852.
9 T. P. Kainulainen, P. Erkkilä, T. I. Hukka, J. A. Sirviö and J. P. Heiskanen, *ACS Appl. Polym. Mater.*, 2020, **2**, 3215–3225.
10 Y. Sun, Z. Zhou, H. Jiang, Y. Duan, J. Li, X. Liu, L. Hong and C. Zhao, *Dent. Mater.*, 2022, **38**, 281–293.
11 S. Wang, Y. Wu, J. Dai, N. Teng, Y. Peng, L. Cao and X. Liu, *Eur. Polym. J.*, 2020, **123**, 109439.
12 J.-T. Miao, S. Peng, M. Ge, Y. Li, J. Zhong, Z. Weng, L. Wu and L. Zheng, *ACS Sustainable Chem. Eng.*, 2020, **8**, 9415–9424.
13 K. Schröder, K. Matyjaszewski, K. J. T. Noonan and R. T. Mathers, *Green Chem.*, 2014, **16**, 1673–1686.
14 A. Kokel and C. Schäfer, Application of Green Chemistry in Homogeneous Catalysis, *Green Chem.*, 2018, 375–414. Elsevier, ISBN 9780128092705.
15 Z. Wang, Y. Hu and J. Yu, Anaerobic sealant and preparation method thereof, CN115160962A, 2022, A China National Intellectual Property Administration.
16 I. S. Sirotin, E. A. Gorbunova, V. Xuan-Son, D. V. Onichin and V. V. Kireev, Phosphase-containing oligoester acrylate and method for its production, RU2743697C1, 2019, Federal Service for Intellectual Property (Rospatent).
17 J. Hao, Silane coupling agent containing hydroxyl group and (methyl) acryloyloxy, CN113968879A, 2021, A China National Intellectual Property Administration.
18 L. Wang, J. Xiao and Y. Wu, High-weather-resistance water-based modified polyacrylic acid bridge concrete protective coating, CN116463022A, 2023, A China National Intellectual Property Administration.
19 W. Shan, W. Li, H. Wang, Q. Zhang, Z. Hua and X. Han, Hexa-functional group polyurethane acrylate containing triazine ring, and preparation method and application thereof, CN110872372A, 2020, A China National Intellectual Property Administration.
20 H. Irie and O. Shibata, Active energy ray-curable resin composition and concrete protection material, JP2023000195A, 2023, Japan Patent Office.
21 Y. Chen, Resin composition, glue dripping material, glue pressing material and preparation methods and application of glue dripping material and glue pressing material, CN113004855A, 2021, A China National Intellectual Property Administration.
22 P. J. Homnick, T. P. Klun, B. R. Pietz, C. S. Lyons and K. K. Stensvad, Fluorinated coupling agents and fluorinated

(co)polymer layers made using the same, WO2021229338A1, 2021, World Intellectual Property Organization.

23 S. Wang, X. Liu, J. Lu, L. Chen, T. Sun and W. Yao, Photosensitive polypropylene material and preparation method thereof, CN114085457A, 2022, A China National Intellectual Property Administration.

24 B. Ren and T. Guan, Polymerizable polyurethane associative thickener with side group at tail end as well as preparation method and application of polymerizable polyurethane associative thickener, CN111944112A, 2020, A China National Intellectual Property Administration.

25 H. Fan, J. Zheng, Y. Cai, X. Liang and J. Wei, Ultraviolet light-thermocuring composition for 3D printing and application of ultraviolet light-thermocuring composition, 112794943A, 2021, *A China National Intellectual Property Administration*.

26 F. Xu, S. Wang, Y. Li, X. Ding and Y. Dong, Cationic softening agent and preparation method and application thereof, CN113373690A, 2021, A China National Intellectual Property Administration.

27 P. Desai and R. N. Jagtap, Photo-curable multifunction acrylated/methacrylated epoxy resin and one-pot preparation thereof, 2022153095A1, 2022, *World Intellectual Property Organization*.

28 S. H. Koo, C. Y. Boo, H. I. Kim, J. H. Bang, S. H. Yang, S. H. Han and H. S. Yeo, Novel glyceride compound and preparation method thereof, WO2022260401A1, 2022, World Intellectual Property Organization.

29 Y. Miyamoto, M. Kamiya, M. Aburano and J. M. Yatvin, Lithographic printing plate precursor and method of use, WO2022051095A1, 2022, World Intellectual Property Organization.

30 X. Zhang, M. Han and J. Wang, Preparation of cationic surfactants, US2022033348A1, 2022, United States Patent and Trademark Office.

31 L. Ning and D. Peng, Electronic material and use thereof, CN110713616A, 2020, A China National Intellectual Property Administration.

32 A. Gu, L. Ning, G. Liang and L. Yuang, Remoldable bismaleimide resin and application thereof, WO2021018158A1, 2021, World Intellectual Property Organization.

33 J. Xie, Preparation method of ultraviolet-cured waterborne polyurethane containing HMMM resin type diol, CN112375204A, 2021, A China National Intellectual Property Administration.

34 K. Satake, K. Asai, K. Sunahara and Y. Satake, Polymer material, WO2020175382A1, 2020, World Intellectual Property Organization.

35 S. Yamada and Y. Kameyama, Epoxy (meth)acrylate resin composition, curable resin composition, cured product, and article, JP2021055005A, 2021, Japan Patent Office.

36 M. Kiguchi, T. Harada and R. Ogiwara, Two-liquid curable coating agent and multilayer film, JP2022136407A, 2022, Japan Patent Office.

37 Y. Sawai, K. Mishima, N. Miyashita and T. Yamakawa, Photosensitive colored composition, cured object, banks, organic electroluminescent element, and image display device, WO2022176976A1, 2022, World Intellectual Property Organization.

38 M. Liu, J. Xu, G. Lin, W. Tu and Q. Ding, UV-curable water-based cathode electrophoretic coating as well as preparation method and application thereof, CN113801565A, 2021, A China National Intellectual Property Administration.

39 J. Zhang, Y. Long, J. Chen and Y. Wang, Curable resin and liquid crystal sealant prepared from same, CN116217892A, 2023, A China National Intellectual Property Administration.

40 T. Robert and S. A. Pérocheau, Process for producing free-radically curable compositions based on novel reactive diluents and reactive diluents, WO2022058473A1, 2022, World Intellectual Property Organization.

41 T. Yuan, H. Wu, J. Huang, J. Zhang and Z. Yang, Bio-based multifunctional flame-retardant epoxy acrylate as well as preparation method and application thereof, CN113292910A, 2021, A China National Intellectual Property Administration.

42 J. Miao, L. Wu, M. Ge, S. Peng and L. Zheng, Bio-based 3D printing resin and preparation method thereof, CN113583165A, 2021, A China National Intellectual Property Administration.

43 J. Dai, S. Wang, X. Liu and J. Zhu, Light-cured resin based on organic polyatomic acid as well as preparation method and application of light-cured resin, CN111978444A, 2020, A China National Intellectual Property Administration.

44 X. Xia, D. Lin, X. Wan, Y. Hong, Y. Chen, J. Han, J. Cai and T. Chen, Isocyanate-based epoxy resin rust-inhibitive primer, CN113637388A, 2021, A China National Intellectual Property Administration.

45 (*a*) **https://echa.europa.eu/registration-dossier/-/registered-dossier/14938/2/1**, accessed 14.10.23 (*b*) **https://www.sigmaaldrich.com/NL/en/sds/vetec/v000751**, accessed 29.10.23.

46 (*a*) **https://echa.europa.eu/registration-dossier/-/registered-dossier/15982/2/1**, accessed 14.10.23 (*b*) **https://www.sigmaaldrich.com/NL/en/sds/mm/8.18839**, accessed 29.10.23.

47 (*a*) **https://echa.europa.eu/registration-dossier/-/registered-dossier/13659/2/1**, accessed 14.10.23 (*b*) **https://www.sigmaaldrich.com/NL/en/sds/mm/8.08270**, accessed 29.10.23.

48 (*a*) D. Tong, J. Chen, D. Qin, Y. Ji, G. Li and T. An, *Sci. Total Environ.*, 2020, **737**, 139830; (*b*) **https://echa.europa.eu/en/registration-dossier/-/registered-dossier/14938/2/1**, accessed 03.12.2023 (*c*) **https://www.sigmaaldrich.com/NL/en/sds/mm/8.08352?userType=anonymous**, accessed 03.12.2023.

49 S. Chen, L. Artiglia, F. Orlando, J. Edebeli, X. Kong, H. Yang, A. Boucly, P. C. Arroyo, N. Prisle and M. Ammann, *ACS Earth Space Chem.*, 2021, **11**, 3008–3021.

50 M. A. Johnson, J. D. Reedy and K. Yang, Method for preparing tetrabutylammonium bromide, US3965178A, 1976, United States Patent and Trademark Office.

51 X. Gong, J. Li, H. Li, W. Wang and Y. Cui, Synthesis method of tetrabutylammonium bromide, CN116023269A, 2023, A China National Intellectual Property Administration.
52 A. Zhu, H. Zhou and L. Jin, Triphenylphosphine, CN108178773A, 2018, A China National Intellectual Property Administration.
53 S. Guangri, B. Caifeng and S. Youmei, Synthesis of triphenyl phosphine, CN1069273A, 1993, A China National Intellectual Property Administration.
54 W. Liu, P. Lu and C. Chen, Positive working photosensitive material, WO2020048957A1, 2020, World Intellectual Property Organization.
55 M. Wang, X. Jian, J. Wang, Y. Zou, L. Zong, Z. Bi and C. Tang, Preparation method of high-refractive-index anti-blue-light modified epoxy acrylate material and optical filter, CN116023813A, 2022, A China National Intellectual Property Administration.
56 Y. Zhang, X. Fan, X. Fan and K. Lu, High-toughness glass fiber and preparation method thereof, CN114606771A, 2022, A China National Intellectual Property Administration.
57 Y. Yu, C. Zhou, H. Ying, J. Liu and P. Chen, Synthesis method of benzyltriethylammonium chloride, CN115521209A, 2022, A China National Intellectual Property Administration.
58 L. Sun, T. Yang, H. Li and Y. Lou, Preparation method of glycidyl tertiary carboxylic ester, WO2013097724A1, 2013, World Intellectual Property Organization.
59 M. Imai, K. Sugimoto, K. Fuji, A. Otsuji, T. Okhuma, M. Takagi, R. Suzuki and K. Takuma, Sulfur-containing unsaturated carboxylate compound and its cured products, US6458908B1, 2000, United States Patent and Trademark Office.
60 M. Paradas-Palomo, S. Flores-Penalba, J. Garcia-Miralles, H.-G. Kinzelmann, R. M. P. Sebastián, J. C. Marquet, J. C. Aguilera, F. Ariolo and T. Hemery, Method for producing functionalized polyesters, WO2018206181A1, 2018, World Intellectual Property Organization.
61 D. Yea, L. Yejin, K. Park and J. Lim, *J. Ind. Eng. Chem.*, 2021, **97**, 287–298.
62 G. Merfeld, C. Molaison, R. Koeniger, A. Ersin Acar, S. Mordhorst, J. Suriano, P. Irwin, R. S. Warner, K. Gray, M. Smith, K. Kovaleski, G. Garrett, S. Finley, D. Meredith, M. Spicer and T. Naguy, *Prog. Org. Coat.*, 2005, **52**, 98–109.
63 W. J. Blank, Z. A. He and M. Picci, *J. Coat. Technol.*, 2002, **74**, 33–41.
64 S. Behrouz, M. N. S. Rad, M. A. Piltan and M. M. Doroodmand, *Helv. Chim. Acta*, 2017, **100**, e1700144.
65 A. E. Gurgiolo, Process for preparation of β-hydroxy esters by reaction of organic carboxylic acids and vicinal epoxides, US4069242A, 1978, United States Patent and Trademark Office.
66 Y. Zhao, W. Wang, J. Li, F. Wang, X. Zheng, H. Yun, W. Zhao and X. Dong, *Tetrahedron Lett.*, 2013, **54**, 5849–5852.
67 (*a*) **https://echa.europa.eu/registration-dossier/-/registered-dossier/13681/2/1**, accessed, 29.10.23 (*b*) **https://www.sigmaaldrich.com/NL/en/sds/sial/270970**, 29.10.23.
68 Y. Grosse, D. Loomis, K. Z. Guyton, F. E. Ghissassi, V. Bouvard, L. Benbrahim-Tallaa, H. Mattock and K. Straif, *Lancet Oncol.*, 2017, **18**, 1003–1004.
69 D. H. Stuermer, D. J. Ng and C. J. Morris, *Environ. Sci.*, 1982, **16**, 582–587.
70 A. M. Bond, R. J. H. Clark, D. G. Humphrey, P. Panayiotopoulos, B. W. Skelton and A. H. White, *J. Chem. Soc., Dalton Trans.*, 1998, **11**, 1845–1852.
71 F. F. Moreira, T. Hasegawa, D. J. Evans and F. S. Nunes, *J. Coord. Chem.*, 2007, **60**, 185–191.
72 Y. Li, J. J. Wilson, L. H. Do, U.-P. Apfel and S. J. Lippard, *Dalton Trans.*, 2012, **41**, 9272–9275.
73 C. D.-T. Nielsen and J. Burés, *Chem. Sci.*, 2019, **10**, 348–353.
74 (*a*) **https://echa.europa.eu/registration-dossier/-/registered-dossier/17217/2/1**, accessed 24.02.2023 (*b*) **https://www.sigmaaldrich.com/NL/en/sds/mm/8.51055**, accessed, 29.10.23.
75 B. Marescau, D. R. Deshmukh, M. Kockx, I. Possemiers, I. A. Qureshi, P. Wiechert and P. P. De Deyn, *Metabolism*, 1992, **41**, 526–532.
76 A. Gobbi and G. Frenking, *J. Am. Chem. Soc.*, 1993, **115**, 2362–2372.
77 C. A. Seipp, M. J. Williams, M. K. Kidder and R. Custelcean, *Angew. Chem., Int. Ed.*, 2016, **56**, 1042–1045.
78 S. Li and C. Lanzhen, Process for synthesizing guanidine carbonate, CN1560031A, 2005, A China National Intellectual Property Administration.
79 D. Prat, A. Wells, J. Hayler, H. Sneddon, C. R. McElroy, S. Abou-Shehada and P. J. Dunn, *Green Chem.*, 2016, **18**, 288–296.
80 S. Guancheng and H. Guoyu, Method for preparing tetraphenyl phosphoric bromide, CN101418014A, 2009, A China National Intellectual Property Administration.
81 M. Trujillo-Lemon, K. L. Wall and K. Esquibel, Carbamate-methacrylate monomers and their use in dental applications, US20100307378A1, 2010, United States Patent and Trademark Office.
82 S. Matsumoto, Photosensitive resin composition, JP2021117442A, 2021, Japan Patent Office.
83 Y. Gao, Y. Wen, C. Zeng, F. Wang, J. Wang, M. Liu, Y. Bi, Q. Liu, S. Yan and J. Luo, Phenolic aldehyde modified mud-resistant polycarboxylate superplasticizer and preparation method thereof, CN111560092A, 2020, A China National Intellectual Property Administration.
84 L. G. Wade, *Organic Chemistry, Pearson new international ed.*, 2013, Pearson Education Limited, Harlow, p. 985.
85 A. Schoeters, Loop oxidation of toluene to benzoic acid, WO2017017524A1, 2017, European Patent Office.
86 Y. P. Wijaya, I. Kristianto, H. Lee and J. Jae, *Fuel*, 2016, **182**, 588–596.

87 T. Dai, C. Li, B. Zhang, H. Guo, X. Pan, L. Li, A. Wang and T. Zhang, *ChemSusChem*, 2016, **9**, 3434–3440.
88 A. M. Niziolek, O. Onel, Y. A. Guzman and C. A. Floudas, *Energy Fuels*, 2016, **30**, 4970–4998.
89 A. del Olmo, J. Calzada and M. Nuñez, *Crit. Rev. Food Sci. Nutr.*, 2017, **57**, 3084–3103.
90 **https://www.food.gov.uk/business-guidance/approved-additives-and-e-numbers**, accessed 10.07.23.
91 J. Davidson and J. A. Le Clerc, *J. Agron*, 1917, **9**, 145.
92 E. Wildermuth, H. Stark, G. Friedrich, F. L. Ebenhöch, B. Kühborth, J. Silver and R. Rituper, *Iron Compounds, in Ullmann's Encyclopedia of Industrial Chemistry*, 2000, Wiley-VCH, Weinheim..
93 T. Walligmann, M. Tokarska-Schlattner, D. Neumann, R. M. Epand, R. F. Epand, R. H. Andres, H. R. Widmer, T. Hornemann and V. Saks, *Molecular System Bioenergetics: Energy for Life*, *Wiley-VCH*, 2007.
94 E. Schulze and E. Steiger, *Biol. Chem.*, 1887, **11**, 43–65.
95 B. Wang, T. Dong, A. Myrlie, L. Gu, H. Zhu, W. Xiong, P. Maness, R. Zhou and J. Yu, *Green Chem.*, 2019, **21**, 2928–2937.
96 A. Schmidt, K. Wegleitner, J. H. Hatzl, R. Sykora and F. Weinrotter, Process for the preparation of guanidine carbonate, US3952057A, 1972, United States Patent and Trademark Office.
97 J. M. Lee, Process for manufacturing melamine from urea, US5384404A, 1993, United States Patent and Trademark Office.
98 H. Gabriel and R. Dicke, Method for increasing the guanidine carbonate yield in a combined melamine process and guanidine carbonate treatment process, EP3626706A1, 2020, European Patent Office.
99 P. T. Browning, Hair Relaxer, WO2003039291A2, 2003, World Intellectual Property Organization.
100 **https://echa.europa.eu/assessment-regulatory-needs/-/dislist/details/0b0236e1873b78fe**, accessed, 24.02.2023.